PATH-INTEGRAL SIMULATION OF PURE WATER [☆]

A. WALLQVIST and B.J. BERNE
Department of Chemistry, Columbia University, New York, NY 10027, USA

Received 6 March 1985; in final form 23 April 1985

Path-integral techniques are used to study the quantum effects on the translational degrees of freedom of both liquid water at 300 K and small clusters ($n = 1,2,3$) at 100 K. Quantum structural effects are small but consistent for liquid water, whereas significant effects are observed in the clusters.

1. Introduction

Classical molecular dynamics (MD) and Monte Carlo (MC) simulations have contributed much to the present understanding of water; nevertheless these classical model systems tend to overestimate the tetrahedral structure of liquid water. Because the H_2O molecule has a low moment of inertia it is expected that in low-temperature clusters, as well as in room-temperature liquid, quantum effects will allow the molecules to librate into classically forbidden regions, thus reducing the strong directionality of the hydrogen bonding. In this Letter we present the results of a quantum-mechanical computer simulation of the moieties $(H_2O)_1$, $(H_2O)_2$ and $(H_2O)_3$ at 100 K, and of liquid water at 300 K. A modified central-force potential model is used with the property that the water molecules are flexible and can vibrate.

The simulations are based on the path-integral formulation of quantum statistical mechanics [1–4]. In this formulation a quantum particle (the H and O atoms) is represented by a cyclic chain polymer containing P classical pseudoparticles connected by nearest neighbor harmonic potentials. The chains representing two different quantum particles interact such that bead j on chain a interacts with bead j on chain b through $V(|r_{aj} - r_{bj}|)/P$ where $V(|r|)$ is the interaction potential of the two quantum particles. Ignoring exchange, the total potential is then given by $\Sigma_{j=1}^{P} V(|R_{aj} - R_{bj}|)/P$, and the inter-particle potential energy of the many-body system is represented by a sum over all pairs of chains. In the limit $P \to \infty$ one recovers the exact results; however in a simulation one has to choose a finite P. The lower the temperature, the higher P must be to give accurate results. For intramolecular vibrations of H_2O at room temperature, $\beta\hbar\omega \gg 1$ (where ω represents any of the vibrations of the H_2O molecule), and P must be large to accurately simulate quantum H_2O.

Path-integral methods have been used recently to explore many problems of interest to chemists. In particular the solvation of electrons in fused salts [5], the quantum effects on the structure of liquid neon [6] and argon clusters [7], solvation of H atoms and muonium in classical water [8], solvent effects on tunneling [9], and electronic and vibrational spectra of molecules [10–12] have been addressed by various methods based on path integrals. Recently, Kuharski and Rossky have simulated rigid quantum ST2 liquid water at room temperature [13].

In this paper we employ both path-integral molecular dynamics (PIMD) and Monte Carlo (PIMC) methods to simulate quantum water. We find that the structures of liquid water and water oligomers are changed by quantum dispersion. The computational procedure is first described and followed by a discussion of the results.

[☆] This work was supported by grants from The National Science Foundation and the National Institutes of Health and by a grant of supercomputer time by the NSF Office of Advanced Scientific Computing.

2. Methods

The model used for flexible water is a central force [14] potential with the internal vibrations modeled by a set of Morse potentials [15,16]*. The discretized path-integral method was used in the primitive algorithm [6]. By using a non-rigid water model, the formal extension from a single quantum particle to a water triad is simple. Cluster calculations at 100 K were made using Monte Carlo with 40 pseudoparticles. Trial simulations with 80 pseudoparticles gave negligible differences in structural properties. A Monte Carlo pass consisted of trial moves of the whole molecule, each center of mass of the atom chain, as well as each pseudoparticle individually. Acceptance ratios for all types of moves varied between 0.3 and 0.7. All cluster simulations were performed on a FPS164 attached processor and each simulation took approximately 2 CPU h.

Molecular dynamics path-integral techniques were used for the liquid. The liquid simulation was carried out with 216 water molecules and 3 pseudoparticles for each atom. Periodic boundary conditions were used with a smooth cutoff [17] for all interactions between 5.5 and 6.0 Å. As pointed out earlier [18] there is an inherent ergodicity problem in the path-integral molecular dynamics method. To overcome the ergodicity problem the velocities were periodically resampled according to a Maxwell—Boltzmann distribution. Even so the molecular dynamics results were slow to converge. These liquid simulations were carried out on a CRAY-1S with a vectorized MD code. The vectorized code ran at 38 ksteps/h classically and at 11 ksteps/h for 3 pseudoparticles; a total of 12 CPU h were used. Both the classical and the path-integral runs used approximately 30 ksteps at 0.25 fs for equilibration, then two runs each of 30 ksteps were done which gave similar results to ensure convergence.

Heat capacities were evaluated for the quantum case. Note that in the evaluation of heat capacities for the quantum case C_V is not given solely by the fluctuations in the energy estimator [4].

3. Results and discussion

3.1. *Clusters at 100 K*

The structure of the water monomer $(H_2O)_1$ can be inferred from the pair correlation functions (PCFs) $g_{OH}(r)$ and $g_{HH}(r)$ given in fig. 1. The peak positions of the quantum system (dashed line) are not shifted from those of the classical system (solid line), but the quantum widths are much larger than the classical widths. This quantum dispersion comes largely from the zero-point motion of the bending mode (H—H) and the bond stretching modes (O—H) Thus quantum $(H_2O)_1$ has the same structure, i.e. the same bond lengths and angles as the classical system, but its vibrational amplitudes are much larger. The kinetic energy as calculated from the primitive estimator [4] (6.11 kcal/mole) was similar to the potential energy (5.69 kcal/mole) in the monomer as predicted by the virial theorem for harmonic forces. The vibrational energy at the lowest energy level, $E=\frac{1}{2}\hbar(2\omega_{OH}+\omega_{HH})$, is 13.23 kcal/mole compared to the total simulated energy of 11.80 kcal/mole. Properly including rotational contributions makes the comparison worse, im-

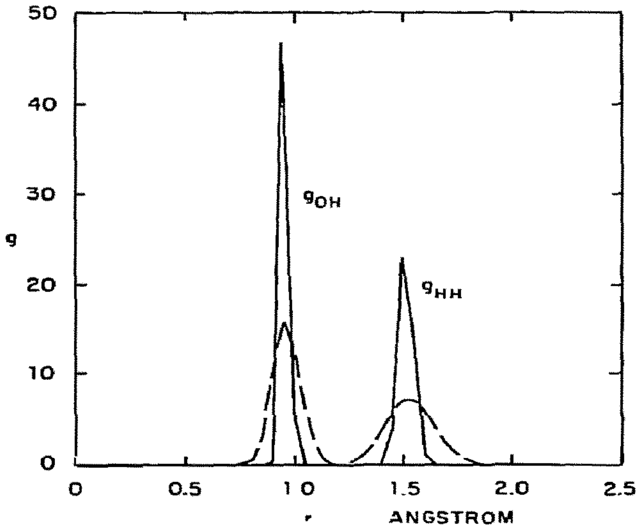

Fig. 1. The pair correlation functions for the constituent atoms in a water monomer at 100 K. Arbitrary units. the first two maxima correspond to the OH bond, the second two maxima to the internal HH distance. Classical: solid line; quantum: broken line.

---

* Note that the dimensionless coordinate S_3 is everywhere erroneously defined as being twice as large as it should be in refs. [15,16].

Table 1
Cluster energies[a)] at 100 K

Configuration	Intermolecular interaction energy $V_{H_2O-H_2O}$	Intermolecular interaction energy V_{H_2O}	Kinetic energy T
monomer			
classical		0.298 ± 0.003 [b)]	
quantum		5.69 ± 0.02	6.11 ± 0.14
dimer			
classical	−2.64 ± 0.01	0.352 ± 0.02	
quantum	−2.38 ± 0.05	5.80 ± 0.06	6.1 ± 0.2
trimer			
SDL			
classical	−3.79 ± 0.05	0.395 ± 0.009	
quantum	−3.493 ± 0.005	5.815 ± 0.005	6.47 ± 0.01
SDC			
classical	−4.83 ± 0.01	0.407 ± 0.003	
quantum	−3.77 ± 0.08	5.80 ± 0.01	6.69 ± 0.03

[a)] All energies reported in kcal/mole.
[b)] Errors are reported as a 95% confidence interval where the standard deviation was calculated assuming a first-order autoregression process using the methods explained by Smith and Wells [19].

plying that either the estimator is poor or the quantum corrections to the internal motion based on $P = 40$ are not sufficient. A feel for the error can be gained by comparing the energy for a harmonic approximation of the oscillation as a function of the number of pseudoparticles with the exact value. For the highest-frequency mode, $\beta\hbar\omega = 52.5$, calculations similar to those presented in ref [4] give $E_{P=40}/E_{\mathrm{exact}} = 0.83$

In the dimer simulations we see from table 1 a significant increase of the intermolecular potential energy In the classical water dimer we infer that two structurally different conformations give rise to the triply split first peak in $g_{HH}(r)$ indicated by the three arrows in fig. 2. Closer examination of some sample configurations reveals that the middle peak corresponds to the energy minimum of the classical dimer [16], and the two adjacent peaks correspond to a slightly tilted dimer where the hydrogen in the hydrogen bond is displaced from the oxygen–oxygen axis.

Structurally we see that the quantum PCFs in fig. 2 for the dimer become more diffuse and shift slightly outward. In contrast to the classical system the quantum $g_{HH}(r)$ for $(H_2O)_2$ does not show any non-equivalent configurations The H in the hydrogen bond has become fully symmetric around the oxygen–oxygen axis. In the quantum $g_{OH}(r)$ we see that the first maxima corresponding to the OH bond has been reduced and broadened. The hydrogen bond has become more diffuse.

For the trimer there are a number of different configurations that can be classified according to how many of the central molecule's hydrogens are engaged in hydrogen bonding. In real life, one is bound to have a mixture of these configurations with lifetimes dependent on the energy barrier separating one conformer from another.

For the systems studied here our terminology follows that of Reimers and Watts [16]. In the single donor linear (SDL) conformer the central molecule has one of its hydrogens engaged in hydrogen bonding, and the two terminal molecules are not hydrogen bonded to each other. This results in a linear configuration. The single donor cyclic (SDC) conformer contains three equivalent water molecules where each molecule has one of its hydrogens engaged in a hydrogen bond. In table 1 it can be seen that the binding energy of the classical SDC trimer is higher than the classical SDL trimer because it has three relatively undisturbed hydrogen bonds. It can also be seen from table 1 that the binding energy for the quantum SDL and SDC trimers is higher than for the corresponding classical trimers. The potential energy of the SDC trimer exhib-

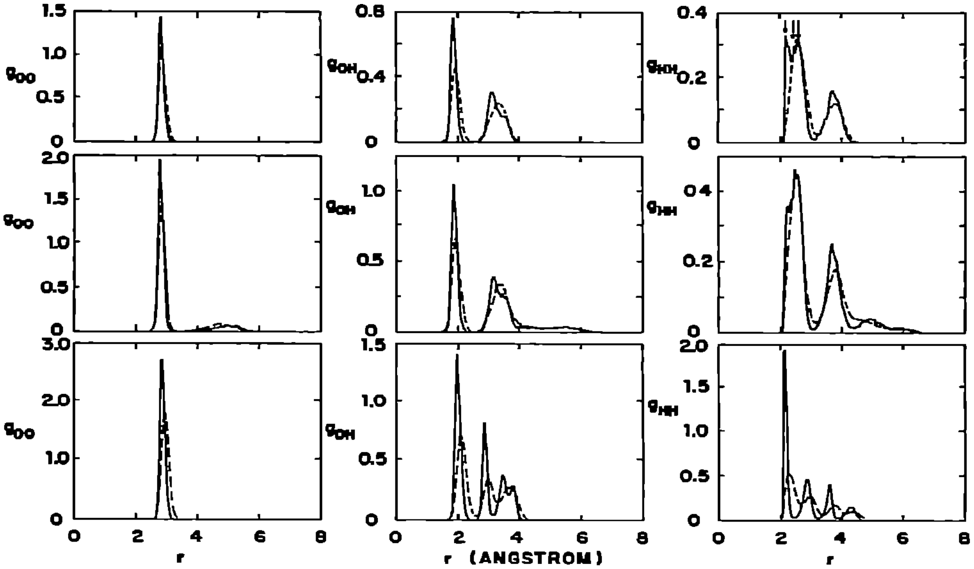

Fig. 2. The pair correlation functions for atoms on different cluster molecules at 100 K. Arbitrary units. From left to right: oxygen–oxygen, oxygen–hydrogen, hydrogen–hydrogen. From top to bottom: dimer, trimer single donor linear (SDL), trimer single donor cyclic (SDC). Classical: solid line; quantum: broken line.

its a larger quantum effect. Quantum mechanics seems to delocalize both arrangements, but the more rigid cyclic arrangement suffers most energetically.

The structure of the SDC trimer is shown in the third row of fig. 2. Here we see that the peak of the g_{OO} is slightly broadened and shifted to larger distances by quantum dispersion. The classically very ordered structure of the HH peaks has been dramatically smoothed out by quantum effects; the hydrogens are allowed to roam larger distances from their equilibrium positions and tunnel into classically forbidden regions of configuration space. In the OH structure we again see many more tunneling configurations though the general structure of the quantum case seems to envelop the classical ones.

For the linear SDL trimer arrangement we observe two maxima in $g_{OO}(r)$, where again the first maximum is slightly broadend and shifted to larger distances. The second maximum is slightly shifted to the left of that for the classical SDL trimer. We believe that this results from quantum tunneling into the repulsive energy barrier separating the linear and cyclic trimers. Comparison of the g_{OH} and g_{HH} corresponding to the dimer and the SDL trimer shows that they are quite similar — as one would expect because the SDL linear arrangement can be viewed as two freely connected dimers.

3.2. *Liquid water*

It is of interest to compare our classical and quantum simulations of liquid water at 300 K and a density of 1.0 g/cm^3. In the quantum system each H and O atom is represented by a three-particle cyclic chain polymer. For the highest frequency mode, $\beta\hbar\omega = 17.5$, calculations as above give $E_{P=3}/E_{\text{exact}} = 0.32$ for a harmonic system. Even though we underestimate the quantum dispersion on the bond lengths and bond angles we believe these effects to be minimal for intermolecular properties.

We first consider how the interaction energy between nearest neighbor water molecules is distributed. The distribution function of these energies is presented in fig. 3a where it can be seen that quantum effects broaden and shift the distribution function toward more repulsive energies. In quantum water many more nearest neighbor pairs interact repulsively than in classical water. In a typical definition of the hydrogen bond

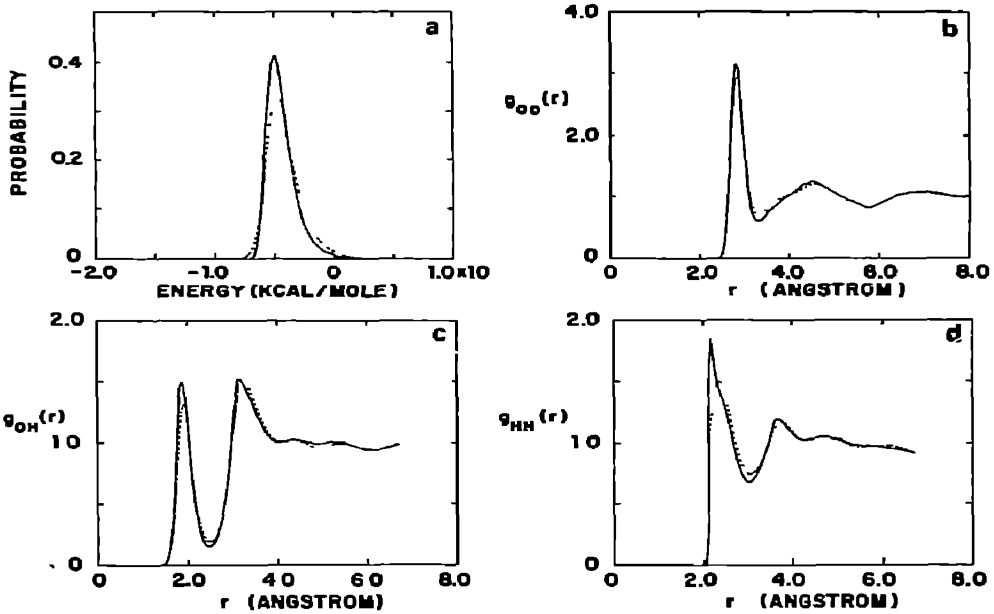

Fig. 3.(a) The nearest neighbor energy distribution for liquid water at 300 K. Classical· solid line; quantum· broken line. (b) The oxygen–oxygen pair correlation function for liquid water at 300 K. Units of g/cm^3. Classical: solid line; quantum. broken line. (c) The oxygen–hydrogen pair correlation function for liquid water at 300 K. Units of g/cm^3. Classical: solid line; quantum. broken line (d) The hydrogen–hydrogen pair correlation function for liquid water at 300 K. Units of g/cm^3. Classical: solid line; quantum: broken line.

two water molecules are said to be hydrogen bonded if their interaction energy is lower than a specified energy V_0, where V_0 is often in the neighborhood of –4 kcal/mole. Fig. 3a shows that for a given choice of V_0 the integrated area of the distribution up to V_0 gives the probability of finding a nearest neighbor pair hydrogen bonded. Fig. 3a shows that this number decreases due to quantum effects, thus the quantum water is less hydrogen bonded than classical water. The quantum distribution extends to lower and higher energies than the classical distribution. The lower energy pairs arise from the ground state vibrational amplitude of the O–H stretch whereas the higher energy pair arise from vibrational tunneling into classically forbidden regions. Ironically, quantum effects can sometimes lead to more structure in the hydrogen bonding.

Table 2 shows that quantum effects shift the potential energies for both the inter- and intra-molecular interactions up from the classical energy minima, with a concomitant decrease in structure. As expected, quantum effects decrease the heat capacity (see table 2) since quantization makes it more difficult to excite the various degrees of freedom. Kuharski and Rossky [13] report a slightly larger decrease in heat capacities. This is probably due to the stated lack of convergence in C_V.

From our point of view, the most important properties of water are the structural properties as seen in the pair correlation functions These PCFs, g_{OO}, g_{OH} and g_{HH}, are also accessible experimentally [20]. Figs.

Table 2
Liquid energies [a] at 300 K

	Classical	Quantum
intermolecular interaction V_{HO-HO}	–10.37 ± 0.02	–9.75 ± 0 04
intramolecular interaction V_{HO}	1.28 ± 0.01	2.81 ± 0.02
C_V [b]	18.6	17.9

[a] Energies reported in kcal/mole.
[b] Heat capacities reported in kcal/mole K.

3b–3d give comparison between the classical and quantum pair correlation functions Small changes in the PCFs of water are observed. The general trend agrees with that of Kuharski and Rossky [13] who studied quantum effects on liquid water containing rigid ST2 molecules. There is a similar softening of the structure with diminished peaks and raised valleys (tunneling) slightly shifted outward. In the OO case (fig 3b) the first peak is slightly lowered and shifted outwards and almost no effect is seen in the second solvation shell. In contrast, in the ST2 simulation of Kuharski and Rossky [13] quantum effects markedly move the second solvation shell out further and broaden it more. This difference seems to be due to the different models of water being studied. Quantum effects shift and broaden the OH and HH peaks (figs. 3c and 3d). The largest effects occur in the first HH peak (fig. 3d) which has been severely reduced. There is little or no effect on the second peak. This effect would appear to be fairly model dependent as hardly any other water model gives such a sharp first classical HH peak. In addition, quantum corrections should be largest for the most sharply peaked quantities.

4. Conclusion

As expected quantum effects are very important in low-temperature clusters. In liquids, quantum effects reduce the hydrogen bonding structures. From these results a set of conjectures can be made about the influence of quantum effect on simulations of aqueous solutions. Given the large dispersion in the quantum-mechanical systems, ionic solutes might be able to distort neighboring water molecules in quantum water much more strongly than in classical water. The quantum reduction of hydrogen bonding in liquid water may have an important effect in reducing hydrophobic interaction and increasing the solubility of hydrophobic molecules.

The quantum simulation of water reported here and elsewhere use pair potential models adjusted to classical simulations of liquid water. It would be desirable to choose a potential optimized on the basis of quantum simulations.

Acknowledgement

We thank Professor P. Rossky for helpful comments on the manuscript. This work would not have been completed were it not for a generous grant of supercomputer time from the Office of Advanced Scientific Computing of the National Science Foundation.

References

[1] R.P. Feynman and R.H. Hibbs, Quantum mechanics and path integrals (McGraw-Hill, New York, 1965).

[2] J.A. Barker, J. Chem. Phys. 70 (1979) 2914.

[3] K S. Schweizer, R.M. Stratt, D. Chandler and P.G. Wolynes, J. Chem. Phys. 75 (1981) 1347.

[4] M.F. Herman, E.J. Bruskin and B.J. Berne, J. Chem. Phys 76 (1982) 5150.

[5] M. Parrinello and A. Rahman, J. Chem. Phys. 80 (1984) 860.

[6] D. Thirumalai, R.W. Hall and B.J Berne, J. Chem. Phys. 81 (1984) 2523.

[7] D.L. Freeman and J.D. Doll, Quantum Monte Carlo Study of the Thermodynamic Properties of Argon Clusters, preprint (1985).

[8] B. De Raedt, M. Sprik and M L. Klein, J. Chem. Phys. 80 (1984) 5719.

[9] D. Thirumalai, E.J. Bruskin and B.J. Berne, J. Chem. Phys 79 (1983) 5063.

[10] D. Thirumalai and J.B. Berne, J. Chem. Phys. 79 (1983) 5029.

[11] D. Thirumalai and B J. Berne, J. Chem. Phys. 81 (1984) 2512.

[12] D. Thirumalai and B.J. Berne, Path Integral Methods Determing Electronic Spectra, preprint (1985)

[13] R.A. Kuharski and P.J. Rossky, Chem. Phys. Letters 103 (1985) 357; A Quantum Mechanical Study of Structure in Liquid H_2O and D_2O, preprint (1985); The Contribution of Intramolecular Vibrations to the Observed Structure of Liquid Water, preprint (1985).

[14] H.L Lemberg and F.H Stillinger, J. Chem. Phys 62 (1975) 1677;
A. Rahman, F.H Stillinger and H.L Lemberg J. Chem. Phys. 63 (1975) 5223;
F.H. Stillinger and A. Rahman, J Chem. Phys. 68 (1978) 666.

[15] J.R. Reimers and R.O. Watts, Chem. Phys. Letters 94 (1982) 222; Chem. Phys 85 (1984) 83.

[16] J.R. Reimers and R.O. Watts, Mol. Phys. 52 (1984) 357.

[17] T.A. Andrea, W.C. Swope and H.C. Andersen, J. Chem. Phys. 79 (1983) 4576

[18] R.W. Hall and B.J. Berne, J. Chem. Phys. 81 (1984) 3641.

[19] E.B. Smith and B.H. Wells, Mol Phys 53 (1984) 701.

[20] A.K. Soper, Chem. Phys. 88 (1984) 187;
W.E. Thiessen and A.H. Narten, J. Chem. Phys 77 (1982) 2656.